

# An estimation of large-signal stability for the bilinear DC-DC converters

**Abstract.** An approach to the analysis of large-signal stability of a Boost converter via the small-signal loop gains is presented. The large-signal stable region of the small-signal designed bilinear Boost converter is estimated in light of the Input-output stability concept. By doing so, the effects of small-signals on large-signal stability are revealed. The effectiveness of the presented approach is verified by simulations and good agreement is reported.

**Streszczenie.** Zaprezentowano analizę stabilności przekształtnika DC-DC typu Boost dla dużych sygnałów. Porównano pracę dla małych i dużych sygnałów i porównano stabilność układów. (Oszacowanie stabilności przekształtników DC-DC typu Boost dla dużych sygnałów)

**Keywords:** Switching power converter, Boost converter, large-signal stability, loop gain

**Słowa kluczowe:** przekształtnik DC-DC typu Boost, stabilność.

## Introduction

The small-signal methods are foundations for analysis and design of switching power converters (SPCs). Relative stabilities of SPCs could be designed based on the small-signal tools, such as Bode, Nyquist plot, and root locus, etc. Although the designed stabilities of SPCs only make sense in the small-signals, they also ensure the large-signal stabilities due to the sufficient stability margins. It is well known that the large-signal stability cannot be predicted by the small-signal models where the approximations made may account much in large-signals. Thus, large-signal analysis is often required to investigate the system convergence behavior under large disturbances, such as input voltage and load current variations.

The virtual equilibrium point approach is proposed by R. Erickson [1] who derived the analytical expressions for the equilibrium points of the system. He also pointed out that the unwanted real equilibria have to be shifted out of the operating region (namely, becoming the virtual equilibria) to ensure the large-signal stable operation of switching regulators. Lyapunov-based approach for design and analysis of the large-signal stability of SPCs was developed by S. Sanders [2] and has been intensively used by other scholars [3-7]. Once the Lyapunov functions have been constructed, the large-signal behavior and stability regions of SPCs could be easily predicted and estimated. Passivity-based methods were also employed for the stability analysis and design of SPCs [8-10]. From the perspective of passivity, the storage function which has the similar form to the Lyapunov type could be generated to design the control laws and stabilities for SPCs. Therefore, both the passivity-based approaches and the Lyapunov-based approaches share the concept of "energy" that used to define the large-signal stabilities for SPCs.

All these approaches for large-signal stability of SPCs were totally different from conventional small-signal methods. The investigations of large-signal stability for SPCs had been conducted independently of small-signal models. Therefore, the connection between the small-signals and the large-signals in SPCs was lost. The effects of small-signals on the large-signal stability have not been well understood yet.

In this paper, the large-signal stability of the switching power converter is analyzed via the small-signal control loops. The effects of small-signal loop gains on the large-signal stability are analytically revealed in light of the Input-Output stability concept. To illustrate the application of the approach, the bilinear Boost DC-DC converter is taken as the case for study throughout the paper.

## Averaging-based modelling

The Boost DC-DC converter (step-up converter) is a well-known switching power converter that is capable of producing the DC output voltage greater than its DC input voltage. Figure 1 shows the Boost DC-DC converter circuit. The input voltage  $V_g$  is step up to a desired output value  $V_o$  with the proper switching on-off of the transistor  $S$  to make the stored energy in the inductor  $L$  power from input voltage  $V_g$  to the output voltage  $V_o$  cyclically.

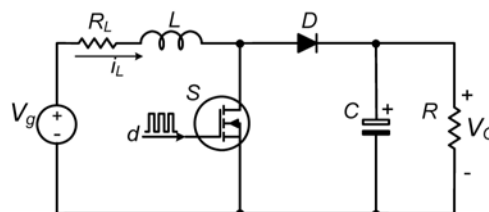


Fig. 1 Boost DC-DC converter circuit

In continuous conduction mode (CCM) of the inductor current  $i_L$ , the transistor  $S$  and the diode  $D$  operate complementarily. The dynamics of the Boost power stage during the power switch  $S$  turn-on and turn-off can be expressed by the following piecewise linear differential equations

$$(1) \quad \begin{cases} \dot{x} = A_1 x + B_1 u, & nT_s \leq t \leq nT_s + dT_s \\ \dot{x} = A_2 x + B_2 u, & nT_s + dT_s \leq t \leq (n+1)T_s \end{cases}$$

where the state vector  $x = \begin{bmatrix} i_L \\ v_o \end{bmatrix}$ , the constant

$$\text{matrices } A_1 = \begin{bmatrix} 0 & 0 \\ 0 & -1/RC \end{bmatrix}, \quad B_1 = \begin{bmatrix} 1/L \\ 0 \end{bmatrix},$$

$$A_2 = \begin{bmatrix} 0 & -1/L \\ 1/C & -1/RC \end{bmatrix} \text{ and } B_2 = \begin{bmatrix} 1/L \\ 0 \end{bmatrix}, \text{ the input matrix}$$

$u = \begin{bmatrix} V_g \\ 0 \end{bmatrix}$ . The variables  $d$  and  $T_s$  are the duty ratio and switching frequency of the Boost power stage respectively.

By using the linear ripple approximation method [11], the above discontinuous model can be approximated by a continuous state-space averaging model

$$(2) \quad \dot{x} = (A_1 d + A_2 d')x + (B_1 d + B_2 d')u$$

The variables in the above equation will be equal to the corresponding quiescent values  $X$  and  $D$  superposed by their perturbations

$$(3) \quad x = X + \hat{x}, \quad d = D + \hat{d}$$

Substituting (3) into (2) produces

$$(4) \quad \dot{\hat{x}}(t) = A\hat{x}(t) + B_0\hat{d} + \hat{x}^T(t)B\hat{d}$$

where

$$A = DA_1 + D'A_2$$

$$B_0 = (A_1 - A_2)X + (B_1 - B_2)V_g$$

$$B = A_1 - A_2$$

It is noted that the (4) describes a bilinear system due to the multiplying term between the state variable and the control input (duty cycle) [12]. Also, the above equation is valid for large signal analysis because no small signal approximation is made. The resulting large-signal perturbation model is also shown in Fig. 2, which can be described as

$$(5) \quad \begin{bmatrix} \dot{\hat{i}}_L \\ \dot{\hat{v}}_O \end{bmatrix} = \begin{bmatrix} -\frac{R_L}{L} & \frac{D'}{L} \\ \frac{D'}{C} & -\frac{1}{R_L C} \end{bmatrix} \begin{bmatrix} \hat{i}_L \\ \hat{v}_O \end{bmatrix} + \begin{bmatrix} \frac{V_O}{L} & 0 \\ 0 & -\frac{I_L}{C} \end{bmatrix} \begin{bmatrix} 1 + \frac{\hat{v}_O}{V_O} \\ 1 + \frac{\hat{i}_L}{I_L} \end{bmatrix} \hat{d}$$

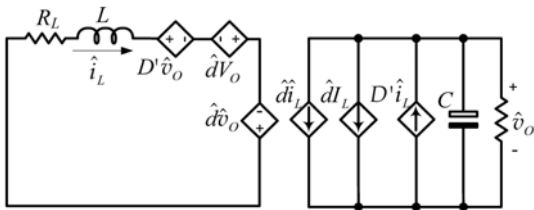


Fig.2 Averaged large-signal perturbation model of the Boost converter circuit

### Compensation of small-signal loop gains

Before embarking on large-signal analysis of the Boost converter, small-signal design of loop gains is necessary to ensure the stability margins. Fig. 3 shows the control block diagram for the average-current mode controlled (ACMC) Boost converter. The ACMC controllers are composed of two compensators: 1) the inner current loop compensator (denoted by  $F_i$ ) to achieve the fast tracking of the inductor current to the reference; 2) the outer voltage compensator (denoted by  $F_v$ ) to force the output voltage following the reference voltage. By this cascaded control structure, the regulation for the converter states is attained at higher dynamics than conventional single control loop structure.

As shown in Fig. 3, the current loop gain and the voltage loop gain are derived as

$$(5) \quad T_i(s) = R_i F_i F_m G_{id}(s)$$

$$(6) \quad T_v(s) = \frac{\beta_v F_v F_m F_i G_{vd}(s)}{1 + T_i(s)}$$

where  $R_i$ ,  $F_m$ ,  $\beta_v$ ,  $G_{vd}(s)$ , and  $G_{id}(s)$  are the current sensor gain, modulator gain, the voltage sensor gain, the duty cycle-to-output voltage transfer function, and the duty cycle-to-inductor current transfer function respectively.

In this design, both the current compensator and the voltage compensator take the two-pole, one-zero compensation network, and their transfer functions are given by

$$(7) \quad F_i(s) = \frac{\omega_i}{s} \cdot \frac{1 + s/\omega_{iz}}{1 + s/\omega_{ip}}$$

$$(8) \quad F_v(s) = \frac{\omega_v}{s} \cdot \frac{1 + s/\omega_{vz}}{1 + s/\omega_{vp}}$$

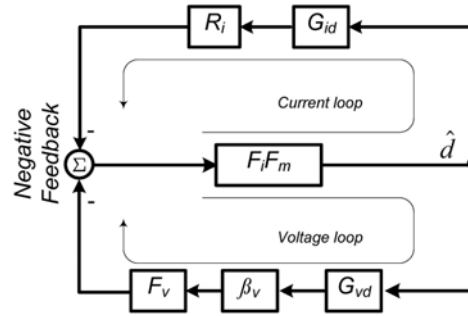


Fig. 3 Control block diagram for the Boost converter

Given the parameters for the Boost converter circuit in Table 1, the designed parameters of the current compensator and the voltage compensator are:  $\omega_i=4900$ ,  $\omega_{iz}=2512$ ,  $\omega_{ip}=125600$ ,  $R_i=0.2$ ,  $F_m=1/3$ , and  $\beta_v=0.042$ ,  $\omega_v=95000$ ,  $\omega_{vz}=630$ ,  $\omega_{vp}=283000$  respectively.

Table 1. The parameters for the Boost converter circuit

Name	Denomination	Values
Filter Inductor	$L$	120 $\mu\text{H}$
Filter Capacitor	$C$	470 $\mu\text{F}$
Nominal load	$R$	60 $\Omega$
Equivalent resistance	$R_L$	150 m $\Omega$
Switching frequency	$f_{sw}$	100 kHz
Input Voltage	$V_g$	36 V
Output Voltage	$V_O$	72 V

The Bode diagram for both the current loop gain and the voltage loop gain are then plotted in Fig. 4, where the cut-off frequencies and phase margins for both the compensated current loop and the voltage loop are 11 kHz and 60 degree, and 3 kHz and 59 degree respectively.

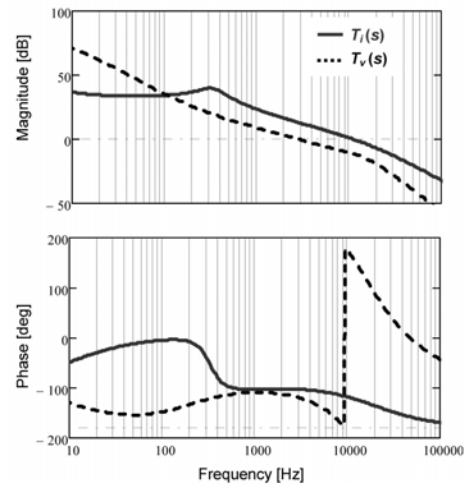


Fig. 4 Compensated loop gains for the Boost converter

### Analysis of Large-signal stability

As the derived equation (4), the state-space averaging representation of the Boost converter results in a bilinear

system which make the Boost converter be subjected to instabilities under large-signal disturbances.

From the control block diagram in Fig. 3, the control input (duty cycle) is derived as

$$(9) \quad \hat{d} = -\beta_v F_v F_m F_i \hat{v}_O - R_i F_m F_i \hat{i}_L + d_z$$

where  $d_z$  represents the input disturbance of the outer voltage control loop.

The large-signal model of the Boost converter in Fig. 2 also gives

$$(10) \quad \hat{i}_L = G_{id} \cdot \left(1 + \frac{\hat{v}_O}{V_O}\right) \cdot \hat{d}$$

$$(11) \quad \hat{v}_O = G_{vd} \cdot \left(1 + \frac{\hat{i}_L}{I_L}\right) \cdot \hat{d}$$

Substituting (10) and (11) into (9), then (9) is rewritten as

$$(12) \quad \hat{d} = -T_v \cdot \left(1 + \frac{\hat{i}_L}{I_L}\right) \cdot \hat{d} - T_i \cdot \left(1 + \frac{\hat{v}_O}{V_O}\right) \cdot \hat{d} + d_z$$

Rearranging the above equation generates

$$(13) \quad \hat{d} = \frac{-T_v}{1+T_v+T_i} \frac{\hat{i}_L}{I_L} \hat{d} + \frac{-T_i}{1+T_v+T_i} \frac{\hat{v}_O}{V_O} \hat{d} + \frac{d_z}{1+T_v+T_i}$$

Application of the Kittaneh's norm inequality [14] which is sharper than the conventional triangular inequality yields (14), shown at the bottom of this page.

And the gain of the system is defined as

$$(15) \quad g(H) = \sup_{u \neq 0, t \geq 0} \frac{\|Hu\|}{\|u\|}$$

Then, the equation (14) is rearranged as (16), shown at the bottom of this page.

$$(14) \quad \|\hat{d}\| \leq \frac{1}{2} \left( g\left(\frac{T_v}{1+T_v+T_i}\right) \frac{|\hat{i}_L|}{I_L} \|\hat{d}\| + g\left(\frac{T_i}{1+T_v+T_i}\right) \frac{|\hat{v}_O|}{V_O} \|\hat{d}\| + \sqrt{\left(g\left(\frac{T_v}{1+T_v+T_i}\right) \frac{|\hat{i}_L|}{I_L} \|\hat{d}\| - g\left(\frac{T_i}{1+T_v+T_i}\right) \frac{|\hat{v}_O|}{V_O} \|\hat{d}\|\right)^2 + 4 \left\| \left(\frac{T_v}{1+T_v+T_i}\right) \frac{|\hat{i}_L|}{I_L} \|\hat{d}\| \right\|^{1/2} \left\| \left(\frac{T_i}{1+T_v+T_i}\right) \frac{|\hat{v}_O|}{V_O} \|\hat{d}\| \right\|^{1/2}} \right) + g\left(\frac{1}{1+T_v+T_i}\right) \cdot \|d_z\|$$

$$(16) \quad \|\hat{d}\| \leq \frac{g\left(\frac{1}{1+T_v+T_i}\right) \cdot \|d_z\|}{1 - \frac{1}{2} \left( g\left(\frac{T_v}{1+T_v+T_i}\right) \frac{|\hat{i}_L|}{I_L} + g\left(\frac{T_i}{1+T_v+T_i}\right) \frac{|\hat{v}_O|}{V_O} + \sqrt{\left(g\left(\frac{T_v}{1+T_v+T_i}\right) \frac{|\hat{i}_L|}{I_L} - g\left(\frac{T_i}{1+T_v+T_i}\right) \frac{|\hat{v}_O|}{V_O}\right)^2 + 4 \left\| \left(\frac{T_v}{1+T_v+T_i}\right) \frac{|\hat{i}_L|}{I_L} \right\|^{1/2} \left\| \left(\frac{T_i}{1+T_v+T_i}\right) \frac{|\hat{v}_O|}{V_O} \right\|^{1/2}} \right)}$$

$$(17) \quad 1 - \frac{1}{2} \left( g\left(\frac{T_v}{1+T_v+T_i}\right) \frac{|\hat{i}_L|}{I_L} + g\left(\frac{T_i}{1+T_v+T_i}\right) \frac{|\hat{v}_O|}{V_O} + \sqrt{\left(g\left(\frac{T_v}{1+T_v+T_i}\right) \frac{|\hat{i}_L|}{I_L} - g\left(\frac{T_i}{1+T_v+T_i}\right) \frac{|\hat{v}_O|}{V_O}\right)^2 + 4 \left\| \left(\frac{T_v}{1+T_v+T_i}\right) \frac{|\hat{i}_L|}{I_L} \right\|^{1/2} \left\| \left(\frac{T_i}{1+T_v+T_i}\right) \frac{|\hat{v}_O|}{V_O} \right\|^{1/2}} \right) > 0$$

It is known that the control duty ratio  $d$  is the constrained control variable in the Pulse-Width Modulated (PWM) switching power converter, which implies the stable operation for the systems. Therefore, the closed loop controlled Boost converter systems is input-output stable [13] if the denominator of (16) satisfies (17), also shown at the bottom of this page.

The equation (17) indicates the sufficient condition for stable operation of the Boost converter control system, which can be used to calculate the maximum disturbances of the converter states, i.e., inductor current and capacitor voltage. The shaded area in Fig. 5 shows the calculated stability region for the Boost converter based on the parameters given in the Table 1, while its center is the operating point. The stability region means that any deviation from the operating point will inevitably converge to it if only the deviation did not exceed the shaded area. Also, there is no doubt that different loop gains produce different large-signal stability regions.

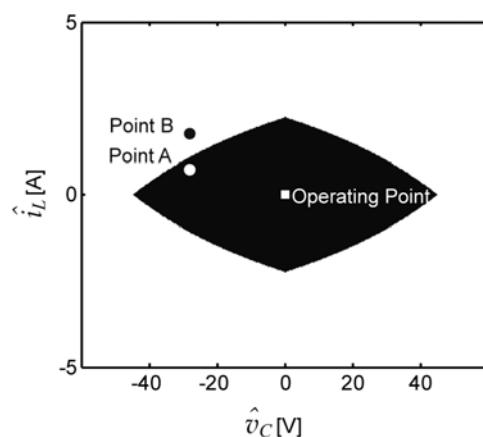


Fig. 5 Stability region for the Closed-loop Boost converter

To verify the effectiveness of the presented approach, two testing point A and B as in Fig. 5, are selected to test the responses of the designed Boost converter under these disturbances. At point B outside the predicted stable region, the disturbance is (+0.8 A, -30 V), which means that there are the positive deviation of 0.8 A for the inductor current and the negative deviation of 30 V for the output voltage at the same time. Also, at point A inside the predicted stable region, the disturbance is (+1.6 A, -30 V), which means that there are the positive deviation of 1.6 A for the inductor current and the negative deviation of 30 V for the output voltage at the same time. The responses of the closed-loop Boost converter to the disturbances of point A and point B are shown in Fig. 6(a) and Fig. 6(b) respectively, where the response of point A is coming into the oscillatory state and the response of point B remains stable after the disturbance. These results agree well with the stability estimation.

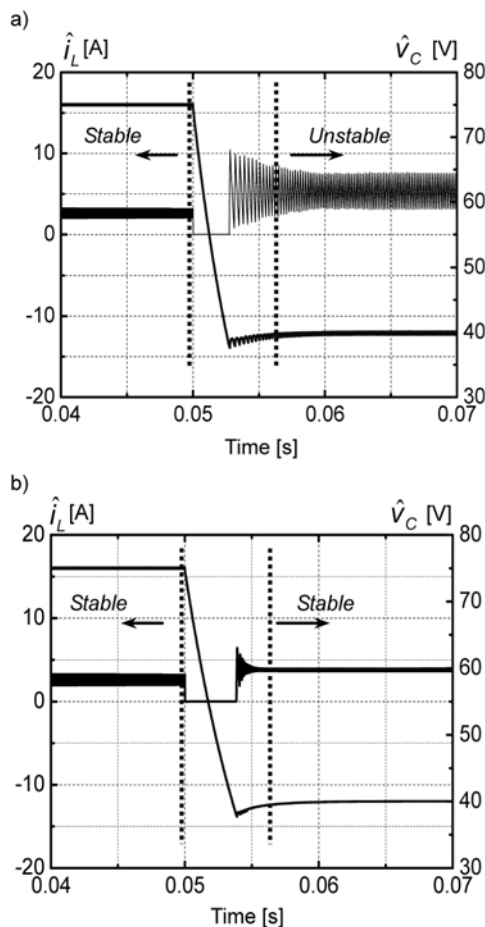


Fig.6. Responses of the Boost converter under different disturbances: (a) unstable response to disturbances of (+1.6 A, -30 V), (b) stable response to disturbances of (+0.8 A, -30 V)

### Conclusion

Analytical approach for the large-signal stability investigation is presented in this paper. By the notion of the Input-output stability, the large-signal stability region for a bilinear DC-DC converter has been estimated via the small-signal loop gains. The effectiveness of the approach has also been verified under different disturbances in the Boost converter. The cornerstone for the analysis and design of SPCs is still the small-signal method. Therefore, the

obtained results could be used for the re-design of the large-signal stability for SPCs.

*Acknowledgments:* This work was supported by the National Science Foundation under grant no. 51137006 and in part by the Fundamental Research Funds for the Central Universities under project no. CDJXS11151151.

### REFERENCES

- [1] Erickson R. W., Cuk S., Middlebrook R. D., Large-signal modelling and analysis of switching regulators, In Proc. 13th Annual IEEE Power Electronics Specialists Conference PESC1982, pages 240-250, 1982.
- [2] Sanders S. R., Verghese G. C., Lyapunov-based control for switched power converters, *IEEE Trans. Power Electron.*, 7(1992), No. 1, 17-24.
- [3] Hu T. S., A Nonlinear-System Approach to Analysis and Design of Power-Electronic Converters With Saturation and Bilinear Terms, *IEEE Trans. Power Electron.*, 26(2011), No. 2, 399-410.
- [4] Sullivan C. J., Sudhoff S. D., Zivi E. L., Zak S. H., Methods of optimal Lyapunov function generation with application to power electronic converters and systems, In Proc. *The IEEE Electric Ship Technologies Symposium ESTS 2007*, pages 267- 274, 2007.
- [5] Almer S., U. Jonsson, Kao C. Y., Mari J., Stability analysis of a class of PWM systems, *IEEE Transactions on Automatic Control*, 52(2007), No. 6, 1072-1078.
- [6] Mazumder S. K., Acharya K., Multiple Lyapunov function based reaching condition analyses of switching power converters, in Proc. *37th IEEE Power Electronics Specialists Conference PESC2006*, pages 1-8, 2006.
- [7] Garcia F. S., Pomilio J. A., Deaecto G. S., Geromel J. C., Analysis and Control of DC-DC Converters Based on Lyapunov Stability Theory, In Proc. *The first IEEE Energy Conversion Congress and Exposition ECCE2009*, pages 2920-2927, 2009.
- [8] Perez M., Ortega R., Espinoza J. R., Passivity-based PI control of switched power converters, *IEEE Transactions on Control Systems Technology*, vol. 12(2004), No. 6, 881-890.
- [9] Leyva R., Cid-Pastor A., Alonso C., Queinnec I., Tarbouriech S., Martinez-Salamero L., Passivity-based integral control of a boost converter for large-signal stability, *IEE Proceedings-Control Theory and Applications*, 153(2006), No. 2, 139-146.
- [10] Jeltsema D., Scherpen J. M. A., A power-based perspective in modeling and control of switched power converters [Past and Present], *Industrial Electronics Magazine, IEEE*, 1(2007), No. 1, 7-54.
- [11] Erickson R. W., Maksimović D., Fundamentals of power electronics, *Kluwer Academic*, 2001.
- [12] Chen F., Cai X. S., Design of feedback control laws for switching regulators based on the bilinear large signal model, *IEEE Transactions on Power Electronics*, 5(1990): 236-240.
- [13] Zames G., On Input-Output Stability of Time-Varying Nonlinear Feedback Systems .I. Conditions Derived Using Concepts of Loop Gain Conicity and Positivity, *IEEE Transactions on Automatic Control*, 11(1966), No.2, 228-238.
- [14] Kittaneh F., Norm inequalities for sums of positive operators, *Journal of Operator Theory*, 48(2002), No. 1, 95-103.

**Authors:** dr. Sucheng Liu, College of Electrical Engineering, Chongqing University, No. 174 Shazhengjie, Shapingba, Chongqing, 400044, China, E-mail: [liusucheng@gmail.com](mailto:liusucheng@gmail.com); prof. dr. Luowei Zhou, College of Electrical Engineering, Chongqing University, No. 174 Shazhengjie, Shapingba, Chongqing, 400044, China, E-mail: [zluowei@cqu.edu.cn](mailto:zluowei@cqu.edu.cn); assoc.prof. dr. Weiguo Lu, College of Electrical Engineering, Chongqing University, No. 174 Shazhengjie, Shapingba, Chongqing, 400044, China, E-mail: [luweiguo@cqu.edu.cn](mailto:luweiguo@cqu.edu.cn).